

# Photodetachment of $[\text{OH}(\text{H}_2\text{O})]^-$

Stephen Golub, and Bruce Steiner

Citation: *The Journal of Chemical Physics* **49**, 5191 (1968); doi: 10.1063/1.1670021

View online: <https://doi.org/10.1063/1.1670021>

View Table of Contents: <http://aip.scitation.org/toc/jcp/49/11>

Published by the American Institute of Physics

---

## Articles you may be interested in

Spectroscopy of the transition state: Elementary reactions of the hydroxyl radical studied by photoelectron spectroscopy of  $\text{O}^-(\text{H}_2\text{O})$  and  $\text{H}_3\text{O}^+_2$

*The Journal of Chemical Physics* **102**, 6088 (1995); 10.1063/1.469343

---

PHYSICS TODAY

WHITEPAPERS

### ADVANCED LIGHT CURE ADHESIVES

Take a closer look at what these environmentally friendly adhesive systems can do

READ NOW

PRESENTED BY  
 **MASTERBOND**  
ADHESIVES | SEALANTS | COATINGS

measured and calculated frequencies using HF constants given by Mann *et al.*<sup>3</sup> and DF constants given by Spanbauer *et al.*<sup>4</sup> The monochromator calibration was verified to  $\pm 0.2 \text{ cm}^{-1}$  with relatively isolated, hence readily identified, lines in HF [ $P_1(4)$  and  $P_1(9)$ ]. The search for other lines was based upon calculated frequencies;  $1\text{-cm}^{-1}$  spectral slitwidths were used for HF and about  $10\text{-cm}^{-1}$  slitwidths for DF. Additional confirmation of the assignments was provided by coincidence measurements between several of the assigned lines and their known counterparts in the  $\text{UF}_6/\text{H}_2(\text{D}_2)$  laser.<sup>5</sup> Table I shows that for HF,  $P_1(4)$  is the first line to reach threshold, but thereafter, each  $P_2(J)$  transition reaches threshold just before the  $P_1(J+1)$  transition that it pumps. DF shows the same pattern of  $P_2(J)$  vs  $P_1(J+1)$  lines, but it is difficult to say whether  $P_1(6)$  or  $P_2(6)$  is the first line to reach threshold. Total laser duration is about  $10\text{--}15 \mu\text{sec}$  and each line has an approximate duration (pressure-dependent) between  $0.5\text{--}5 \mu\text{sec}$ . Preliminary gain measurements indicate that HF and DF have roughly the same gain (if scaled to the same pressure): HF,  $>5\text{db/m}$  at  $4.6\text{-mm}$  sample pressure; DF,  $>2\text{db/m}$  at  $1.4 \text{ mm}$ . Power levels are about  $30\text{--}40\%$  of those of the  $\text{UF}_6/\text{H}_2(\text{D}_2)$  lasers.

Added argon quenches the higher  $P(J)$  lines until, with argon in  $100:1$  excess,  $P_2(6)$ ,  $P_2(7)$ ,  $P_1(4)$ ,  $P_1(6)$ , and  $P_1(7)$  make up the total emission from HF. However, for a moderate excess of argon ( $\sim 10:1$ ), the total emission intensity is approximately doubled. Hexafluoroethane ( $\text{C}_2\text{F}_6$ ) also raises the total intensity, but it produces an additional quenching effect. A  $20:1$  excess of  $\text{C}_2\text{F}_6$  preferentially quenches  $2\rightarrow 1$  HF emission while  $1\rightarrow 0$  lines out to  $P_1(7)$  still emit. With either inert gas present, a single laser tube filling would reach laser threshold in several successive flashes, whereas without inert gas, emission occurred only on the first flash.

We believe that both Ar and  $\text{C}_2\text{F}_6$  act to moderate temperature rise and guarantee rotational equilibration. In addition,  $\text{C}_2\text{F}_6$  is probably quite effective in deactivating the vibrationally excited trifluoroethane. Assuming HF deactivation is negligible (as suggested in earlier work<sup>6</sup>) and that rotational temperature is  $300^\circ\text{K}$ , the observation that  $P_1(4)$  reaches threshold first in HF implies<sup>5</sup> that  $N_1/N_0$  (the population ratio for  $v=1$  and  $v=0$ ) is in the range  $0.58\text{--}0.90$ . A corresponding calculation for DF, assuming  $P_1(6)$  and  $P_2(6)$  emit simultaneously, yields ratios of  $N_1/N_0=0.63\text{--}0.76$  and  $N_2/N_1=0.64\text{--}0.78$ .

The hydrogen fluoride elimination laser is a new type of chemical laser, the first in which a unimolecular chemical reaction provides the pumping mechanism. Other elimination lasers are being sought, and we expect them to be numerous. It seems certain that systematic study of the laser emission dependence upon vibrational deactivation will elucidate the role of vibrational excitation in unimolecular decomposition.

We wish to acknowledge research support from the

U. S. Air Force Office of Scientific Research. Also, we gratefully thank Dr. Eric Whittle for focussing our attention on the potentiality of radical-radical reactions as possible chemical laser sources.

<sup>1</sup>R. D. Giles and E. Whittle, *Trans. Faraday Soc.* **61**, 1425 (1965).

<sup>2</sup>J. V. V. Kasper and G. C. Pimentel, *Appl. Phys. Letters* **5**, 231 (1964).

<sup>3</sup>D. E. Mann, B. A. Thrush, D. R. Lide, Jr., J. J. Ball, and N. Acquista, *J. Chem. Phys.* **34**, 420 (1961).

<sup>4</sup>R. N. Spanbauer, K. N. Rao, and L. H. Jones, *J. Mol. Spectry.* **16**, 100 (1965).

<sup>5</sup>K. L. Kompa, J. H. Parker, and G. C. Pimentel, *J. Chem. Phys.* **49**, 4257 (1968).

## Photodetachment of $[\text{OH}(\text{H}_2\text{O})]^-$ \*

STEPHEN GOLUB† AND BRUCE STEINER

National Bureau of Standards, Washington, D. C. 20234

(Received 13 September 1968)

We have recently come across and begun to study the ion  $[\text{OH}(\text{H}_2\text{O})]^-$ ,<sup>1</sup> whose characteristics indicate that it may play a role in atmospheric physics.<sup>2</sup> In examining the negative ions formed in a hot cathode arc discharge through an ammonia-water vapor mixture at a pressure approximately  $7 \text{ N/m}^2$  ( $0.05 \text{ torr}$ ), we observed (in addition to beams of mass 1, 16, and 17) a  $0.1\text{--}1\text{-nA}$  ion beam at mass 35; at the same time a much weaker beam of mass 37 ions is observed.

The ions formed in this arc are analyzed in a second-order, double-focusing mass analyzer (focusing in velocity spread as well as aperture in the deflection plane).<sup>3,4</sup> Figure 1 shows a mass scan of the region between mass 35 and mass 37. The smaller member of the doublet at mass 35 is seen to be 3 times the main peak at mass 37 as required by the well-known isotopic abundances of  $^{35}\text{Cl}$  and  $^{37}\text{Cl}$ . The mass 35 splitting,  $0.039\pm 0.006 \text{ amu}$ , is equivalent to the  $^{35}\text{Cl}\text{--H}_3\text{O}_2$  mass difference,  $0.044 \text{ amu}$ , and is twice that of either the  $^{35}\text{Cl}\text{--OF}$  or the  $\text{OF}\text{--H}_3\text{O}_2$  mass differences.

The  $\text{H}_3^{16}\text{O}^{18}\text{O}^-$  peak is observed with increased amplification along with the  $^{37}\text{Cl}$  as a second doublet with

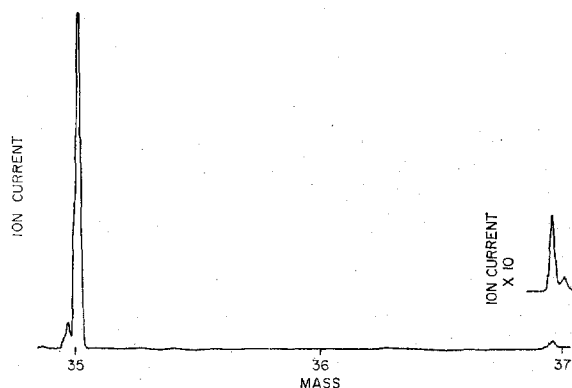


Fig. 1. Mass spectrum of the region containing  $^{35}\text{Cl}^-$ ,  $\text{H}_3^{16}\text{O}_2^-$ ,  $^{37}\text{Cl}^-$ , and  $\text{H}_3^{16}\text{O}^{18}\text{O}^-$ . The insert at mass 37 represents an additional amplification by a factor of 10.

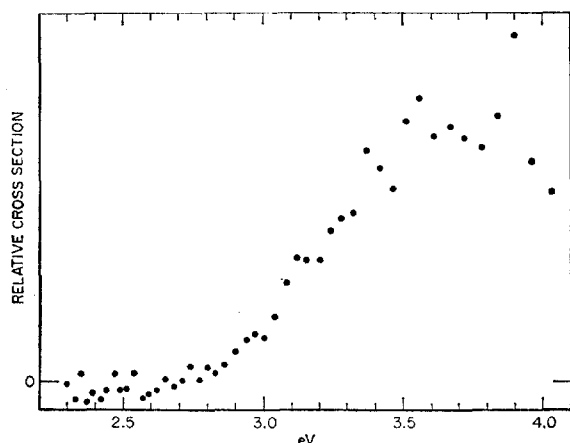


FIG. 2. Relative cross section for photodetachment of  $[\text{OH}(\text{H}_2\text{O})]^-$ . Various slowly varying correction factors have not been applied. The bandwidth was  $20 \text{ nm} \sim 0.14 \text{ eV}$ .

the appropriate mass splitting. The intensity ratio of the peaks identified as  $\text{H}_3^{16}\text{O}^{18}\text{O}^-$  and  $\text{H}_3^{16}\text{O}_2^-$ , 0.004, is appropriate for an ion containing two oxygen atoms.

The  $[\text{OH}(\text{H}_2\text{O})]^-$  beam intersects a resolved photon beam [ $20 \text{ nm}$  ( $200 \text{ \AA}$ )  $\sim 0.14 \text{ eV}$  bandwidth] and the detached electrons are observed. The relative photodetachment cross-section curve ( $\sigma \propto i_{\text{electron}}/i_{\text{ion}}\rho_\lambda$ , where  $i$  is current and  $\rho_\lambda$  is photon flux) for this interaction is shown in Fig. 2. Correction of the observed threshold near  $2.80 \pm 0.15 \text{ eV}$  for the  $20\text{-nm}$  bandwidth yields a corrected threshold of  $2.95 \pm 0.15 \text{ eV}$ . The monotonic rise of the cross section over the full  $1.0 \text{ eV}$  above threshold is in contrast to the behavior of the cross sections for the other two polyatomic negative ions studied in detail,  $\text{OH}^-$ ,<sup>5</sup> and  $\text{SH}^-$ .<sup>6</sup> In these diatomic cases, the structure of the negative ion was found to be sufficiently close to that of the neutral free radical that only one transition between narrow discrete levels was observed. The cross sections rose rapidly over only about  $0.1 \text{ eV}$ .

The structure of neither  $[\text{OH}(\text{H}_2\text{O})]^-$  nor  $[\text{OH}(\text{H}_2\text{O})]$  is known to the authors. The observed detachment cross section rising over  $1 \text{ eV}$  is consistent with a transition from a chemically bound negative ion to a repulsive neutral state which presumably separates into  $\text{H}_2\text{O}$  and  $\text{OH}$ . The electron affinity of  $\text{OH}$  is known to be  $1.8 \text{ eV}$ ,<sup>5</sup> while that of water is considerably less<sup>7</sup>; the lowest-energy negative-ion dissociation process therefore probably leads to  $\text{H}_2\text{O}$  and  $\text{OH}^-$ , so that approximately  $1.2 \text{ eV}$  is to be divided between the chemical binding energy of  $\text{H}_3\text{O}_2^-$  and the kinetic energy of the separating neutral particles after detachment.

Since the main noise source in this experiment is from collisional detachment of the negative ions, the signal-to-noise ratio is a measure of the ratio of photodetachment to collisional-detachment cross sections. This ratio is much smaller for  $[\text{OH}(\text{H}_2\text{O})]^-$  than for other strongly bound negative ions such as  $\text{I}^-$ . A crude estimate of the collisional detachment cross section

obtained by visual observation of the background pulse rate is  $\sim 5 \times 10^{-15} \text{ cm}^2$ .

\* This Research was supported in part by the Advanced Research Projects Agency of the U.S. Department of Defense under the Strategic Technology Office.

† NRC-NBS Postdoctoral Research Associate at the National Bureau of Standards, 1967-1968.

<sup>1</sup> J. L. Moruzzi and A. V. Phelps, *J. Chem. Phys.* **45**, 4617 (1966).

<sup>2</sup> R. E. LeVier and L. M. Branscomb, *J. Geophys. Res.* **73**, 27 (1968).

<sup>3</sup> B. Steiner, *Phys. Rev.* (to be published).

<sup>4</sup> B. Steiner, N. Wells, and R. A. Mills (unpublished).

<sup>5</sup> L. M. Branscomb, *Phys. Rev.* **148**, 11 (1966).

<sup>6</sup> B. Steiner, *J. Chem. Phys.* **49**, 5097 (1968).

<sup>7</sup> P. Gray and T. C. Waddington, *Proc. Roy. Soc. (London)* **A235**, 481 (1956).

## Projection of Diatomic Differential Overlap: Least-Squares Projection of Two-Center Distributions onto One-Center Functions\*

M. D. NEWTON,<sup>†</sup> N. S. OSTLUND,<sup>‡</sup> AND J. A. POPE

*Department of Chemistry, Carnegie-Mellon University,  
Pittsburgh, Pennsylvania 15213*

(Received 16 September 1968)

We report a rapid, general method for approximating the two-, three-, and four-center potential-energy integrals over atomic orbitals ( $\chi_m^A \equiv m\text{th AO on center A}$ ) associated with LCAO MO calculations. The method, referred to as the PDDO method (projection of diatomic differential overlap), has been employed in extensive SCF MO calculations, and good agreement with accurate results demonstrated for over-all molecular properties. The approach is easily generalized to any AO basis set, but will be illustrated for first-row minimum-basis-set Slater-type orbitals<sup>1</sup> (STO's), with the (trivial) restriction on orbital exponents ( $\alpha$ 's),  $\alpha_{2s} = \alpha_{2p}$ . The PDDO method consists of a least-squares projection of all one-electron distributions ( $\Pi_i^{AB} \equiv \chi_m^A \chi_n^B$ ) onto one-center distribution basis functions,  $\Lambda_k^A$  (and  $\Lambda_k^B$ , if  $A \neq B$ ). The  $\Lambda$ 's are themselves normalized STO's and the set  $\{\Lambda^A\}$  for each atom A consists of (1) the exact basis for all one-center distributions ( $\chi_m^A \chi_n^A$ ), and (2) certain additional STO's to facilitate projection of two-center distributions (see below).<sup>2</sup> Considering the first group, we have for H and He:  $\Lambda_{1s}$ , with exponent  $\beta_{1s} = 2\alpha_{1s}$ , and for Li-Ne,  $\{\Lambda\} = \Lambda_{1s}, \Lambda_{2s}, \dots, \Lambda_{3d_{xy}}, \dots, \Lambda_{3d_{zz}}$ , where  $\beta_{1s} = 2\alpha_{1s}$ ,  $\beta_{2s} = \alpha_{1s} + \alpha_{2s}$ ,  $\dots, \beta_{3d} = 2\alpha_{2p}$ . [If  $\alpha_{2s} \neq \alpha_{2p}$ , an extra  $\Lambda(\Lambda_{3s'})$  is required.] Important features of this choice of  $\{\Lambda\}$  are the following: (1) all irreducible representations of the rotation group included in the basis are completely spanned; (2) all distributions, both one and two center are treated formally alike; (3) the projection of one-center distributions is exact. Thus in contrast with the *unmodified* Mulliken<sup>3</sup> or ZDO<sup>4</sup> approximations, rotational invariance is maintained, and important Coulomb and